Dc corona discharges in CO_2–air and CO–air mixtures for various electrode materials

Marcela Morvová

Institute of Physics, Faculty of Mathematics and Physics, Comenius University, Mlynská dolina F2, 842 15 Bratislava, Slovak Republic

Abstract. Positive and negative dc corona discharges in CO–air and CO_2–air mixtures were applied. Natural humid air was used. The step by step development with time of the formation of gas products after the action of the corona discharge was measured *in situ*. The discharge tube was situated in an IR gas cell. The IR absorption spectra were scanned from the area of the inter-electrode distance in successive time steps of the action of the discharge (about 1 min).

Measurements were performed for three combinations of electrode materials, namely Mo–stainless steel, Mo–brass and Cu–brass. Reflection IR absorption spectra from the surfaces of the electrodes used were scanned after the action of the discharge. The influence of the electrode material on the development with time of the reaction products was observed. Polymer–metal complexes with possible catalytic activity are formed on the surfaces of electrodes. From measurements it resulted that the discharge processes consist of simultaneously acting volume processes of plasmochemical nature (probably initiated by electrons) and electrocatalytic surface processes on electrodes (probably initiated by photons).

1. Introduction

Corona discharges are usually realized in non-uniform gaps such as wire–cylinder and point–to–plane gaps and are operated with dc, ac or pulsed power supplies. Corona discharges have been used from the beginning of this century in precipitation and ozonizer techniques and later as a source of charged particles, especially electrons, for the initiation of chemical reactions. One of the most important uses of corona discharges is their use in electrostatic precipitators [1].

Corona discharges are very suitable for removal of various compounds such as SO_2, NO_x, CO_x and hydrocarbons (VOC) from exhausts [2–8]. Usually the 'carrier gas' for these compounds is the natural air (with 350 ppm CO_2 and about 4% water vapour), synthetic air without CO_2 and H_2O or combustion exhaust (with 2–15% CO_2 and about the same amount of water vapour as CO_2).

It is of vital interest to control not only emissions of NO_x and SO_2, which are the major causes of acid rain, but also emissions of CO_2 (30 Gt per year, 60% of all greenhouse gases), CH_x and N_2O, which may lead to global warming of the atmosphere (the greenhouse effect). The CO_2 level in the atmosphere must not increase above 400 ppm (by volume), the present level is 350 ppm (by volume). To attain this it is necessary to reduce the present level of emission of CO_2 by at least 10% [9]. Many industrial nations made commitments at the 1992

Rio summit to stabilize CO_2 emissions at the level of 1990 by the year 2000. The UN's Intergovernmental Panel on Climate Change recommends a 50% reduction of global CO_2 emissions within the next 50 years.

An important source of CO_2 is traffic (12 Gt per year). The methods based on a corona discharge used for removal of various compounds from internal combustion engines usually have an effect also on carbon dioxide. The influences of various corona discharges on diesel and Otto engine exhausts were published in [10, 29, 36–38].

Investigation of CO_2 decomposition processes in corona discharges in the mixture of CO_2 with air, including homogeneous and heterogeneous processes on the surfaces inside the discharge tubes, are of great interest. Very good results were obtained in a pulsed corona discharge in the presence of granular ferroelectric matter. The volume and surface reactions were studied [4, 11–13, 28]. Many authors are still interested in dc corona discharges. The problem of conversion of CO_2 to CO in dc corona discharges of both polarities was studied in [10, 14–16, 24, 26].

For studying conversion of CO_2 to CO it is very important to know the amounts of positive and negative ions present in the inter-electrode area of the discharge. However, most of the measurements (mass spectrometric) are performed for reduced pressures. From these the most frequent ion at reduced pressures is CO_3^-. With rising pressure the concentration of CO_4^- ions increases and, after the pressure of 4 kPa (30 Torr), these ions begin to
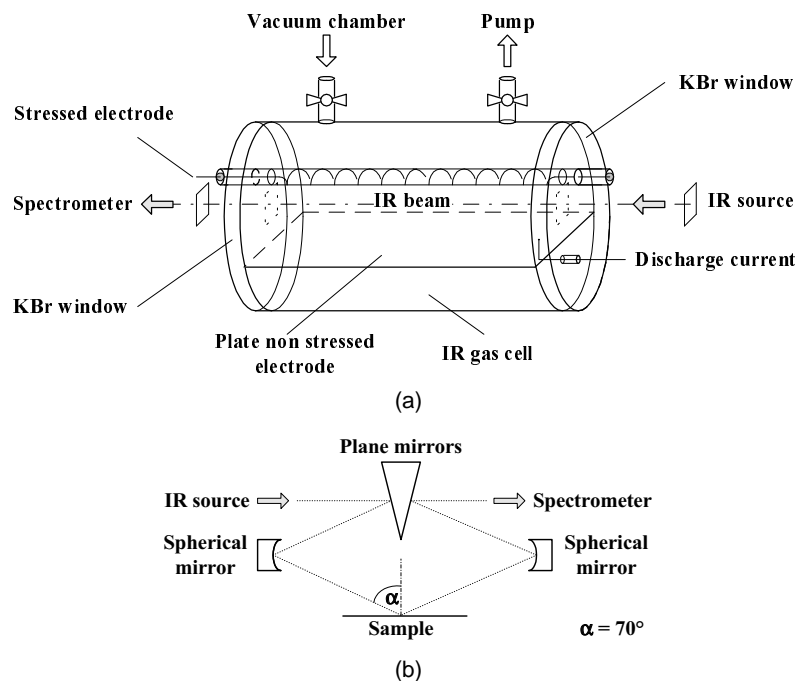
Figure 1. (a) The gas cell corona discharge tube and (b) a schematic diagram of the IR reflection equipment.

dominate. The concentration of cluster ions also rises with increasing pressure. For the negative corona discharge the dominate ions were O^-, CO_3^- and CO_4^-, and those for the positive one were HCO_2^+, CO_2^+ and $H^+[H_2O]_n$ [18, 19]. In the presence of water vapour the surface reactions are very important and lead to the formation of H_2CO_3 [20].

The objective of the present work is to describe

(i) the step by step development with time of the decrease in CO_2 and CO decrease using IR absorption spectrometry;

(ii) the formation of gas products containing stable–NCO radicals and –COO$^-$ and NH_2^+ ions; and

(iii) the corona discharge's self-produced surface catalytic activity of various electrode materials.

2. The experimental set-up and procedure

The experimental apparatus used for *in situ* laboratory measurements and for step by step monitoring of the development with time of product formation consists of

(i) the gas cell corona discharge tube described in figure 1,

(ii) the electrical circuit described in figure 2,

(iii) a gas inlet system and

(iv) auxiliary devices (an IR absorption spectrometer Specord M 80 from Carl Zeiss, an IR gas cell of length 10 cm, reflection equipment, ATR equipment and equipment for the KBr pellet technique).

2.1. The gas cell corona discharge tube

The discharge tubes used were of wire–plane configuration with various electrode materials. The stressed electrode
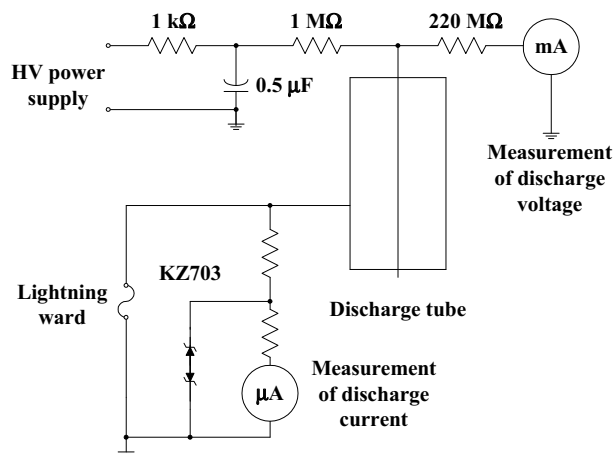
Figure 2. The electrical circuit of the apparatus used.

Table 1. Combinations of electrodes.

Central stressed electrode	Plane non-stressed electrode
Molybdenum	Stainless steel
Molybdenum	Brass
Copper	Brass

was wire of 0.2 mm diameter wound on a glass tube. The non-stressed electrode was a 35 mm × 100 mm plane. To determine the influence of the electrode material on the corona-discharge-affected chemical changes we have used the combination of electrodes in table 1.

The inter-electrode distance was 11 mm. The discharge tube was situated in an IR absorption gas cell so that the

electrodes were parallel to the optical axis of the gas cell, figure 1. This gave the possibility of scanning *in situ* IR absorption spectra from the drift region of the corona discharge along the discharge tube. The IR reflection absorption spectra of the non-stressed plane electrode and IR absorption spectra of deposits on the stressed electrode could also be scanned after the completion of measurements and opening of the discharge tube.

2.2. The electrical circuit of the apparatus

The electrical circuit used is illustrated in figure 2. Two direct-current (positive and negative, 50 Hz rectified by use of a diode) Baur PGK70 high-voltage power sources with 500 W power output, voltage range 0.5–70 kV and maximal current 30 mA were used. The high-voltage dc signal after filtration by a 1 kΩ serially connected resistance and a 0.5 μF parallel connected capacitance was connected to the stressed electrode. The applied voltage was measured by using a milli-ammeter connected via the 200 MΩ resistor to the ground. The current was measured directly from the non-stressed electrode by using a micro-ammeter, protected by a lightning ward and two Zener diodes.

2.3. IR absorption spectrometry

Infrared absorption spectrometry, which is powerful method for identification of various materials in gas, liquid and solid phases, was used for analysis. Carbon dioxide and carbon monoxide are compounds with intense infrared absorption bands. Owing to the action of the electrical plasma, various plasmochemical reactions take place. The final reaction products and intermediates are in many cases unknown. The infrared method is very suitable for their analysis. For analysis we have used various IR techniques and catalogues of IR spectra [40–44] for interpretation.

The gases were analysed in a 10 cm gas cell with KBr or KRS5 windows of similar construction to the gas cell discharge tube described in figure 1. Liquid samples were analysed using the ATR technique with crystals made of KRS5 or Ge, angle of incidence 45° and 60°, sample thicknesses in the range 1.5–5 mm and the crystal length 35 mm.

For solid samples the KBr pellet technique was used. The sample is mixed with the KBr powder in the ratio approximately 0.2–1:100 and they are pulverized together in the vibration mill. The mixture is then pressed under a pressure of 5–22 MPa to the metal ring and in this way the pellet is formed. Spectra from the pellet are scanned.

The electrode's surface was analysed using reflection spectra. The reflection depends on the wavenumber, angle of incidence, refractive index and absorption features of the sample. The device used allows one to measure the reflection spectra at 20° and 70° angles of incidence. Most of the spectra were measured with 70° angle, as shown in figure 1(b).
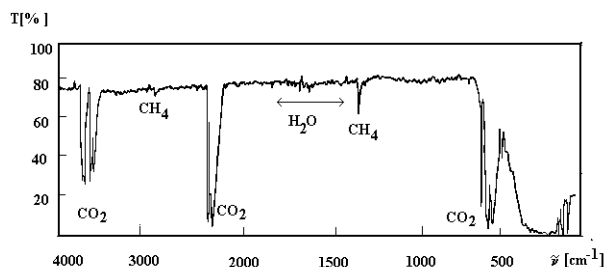
Figure 3. The IR absorption spectrum of CO_2.
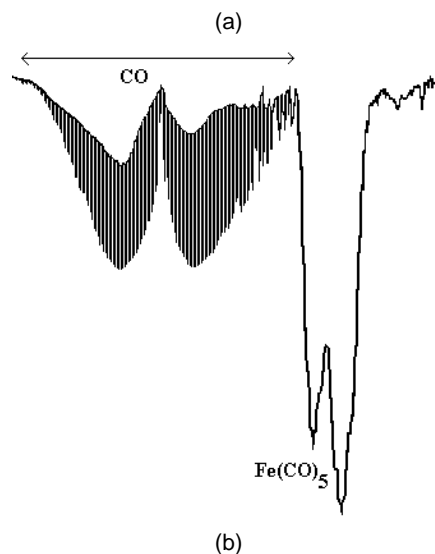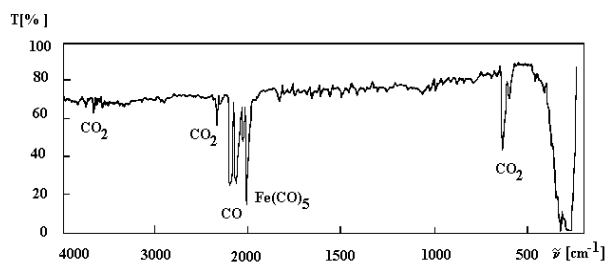
Figure 4. (a) The IR absorption spectrum of CO. (b) Detail of the IR absorption spectrum of CO.

2.4. Gases applied

The CO_2 gas used was of technical grade, contaminated mostly by CH_4 and H_2O, 3.5% together. The IR absorption spectrum of it is in figure 3. The main IR absorption bands of CO_2 are at 670 cm^{-1} (the deformation vibration band), 2350 cm^{-1} (the ν_s stretching vibration) and 3700–3800 cm^{-1} (the cumulative stretching band).

The CO gas used was Matheson with 5% of impurities. The contaminants were $Fe(CO)_5$, which is always present in the pressure tanks with CO to an amount of about 4%, CO_2, about 1%, and H_2O, only traces. The IR absorption spectrum of CO with contaminants is in figure 4(a). CO bands are typical vibration–rotational with the maxima of P and R bands at 2169 and 2115 cm^{-1} (figure 4(b)).

The applied air was not dry. It contained, similarly to natural air, up to 4% of water vapour.

2.5. Measurement procedures

In a gas cell discharge tube we have performed step by step measurements of the development with time of gas phase products and intermediates formed by a discharge in the introduced gas mixture. The infrared spectra from the area of the inter-electrode distance were scanned *in situ*. The studied gas mixture was introduced into the evacuated gas cell–discharge tube as shown in figure 1. The IR spectrum of the introduced gas was scanned. Than the discharge was applied for a defined time and the spectrum was scanned again. This procedure we reiterated until no more changes in composition of the gas took place.

For the introduced CO_2–air mixture the changes of gas product concentration (CO_2 and CO) were studied in time steps 0, 1.5, 3, 4.5, 6 and 16 min. For the introduced CO–air mixture the changes of gas product concentration (CO_2 and CO) were studied in time steps 0, 1, 2, 3 and 4 min. Both positive and negative polarities of the discharge were applied.

After completion of gas phase measurements the non-stressed plate electrode was removed from the gas cell discharge tube and the reflection IR absorption spectrum of it was scanned. From this spectrum it was possible to identify the solid and liquid products on this electrode. The liquid products were additionally analysed by the ATR technique.

During the time of discharge actions considerable changes of gas composition take place. So it was impossible to measure current–voltage characteristics. However, the actual values of the current and voltage were measured and processed in the PC. The applied voltage during the action of the glow corona was about 11 kV and the discharge current was in the range 40–60 μA. When the concentration of CO was high the discharge had a typical glow character. With an enhanced CO_2 concentration the typical glow corona action alternated with a streamer-like spontaneously pulsing discharge with currents up to 300 μA connected with the fall of the voltage to about 1–2 kV.

3. Measurements and discussion of results

3.1. Products created by the action of a discharge in volume

The greatest difference from the point of view of gas composition is that between gas products in positive polarity with electrode materials Mo and stainless steel (figure 5) and negative polarity with electrode materials copper and brass (figure 6). This can be seen from IR absorption spectra. The detailed interpretation of the spectra will be given in section 3.1.2.

3.1.1. Main gas components.
The relative concentrations of CO_2 and CO in percentages of the input concentration for both polarities of a dc corona discharge are shown in figure 7. The time steps used in measurements were 0, 1.5, 3, 4.5, 6 and 16 min for the discharge when a CO_2–air mixture was introduced and 0, 1, 2, 3 and 4 min for the discharge when a CO–air mixture was introduced. Mo–stainless steel, Mo–brass and Cu–brass electrodes were used.
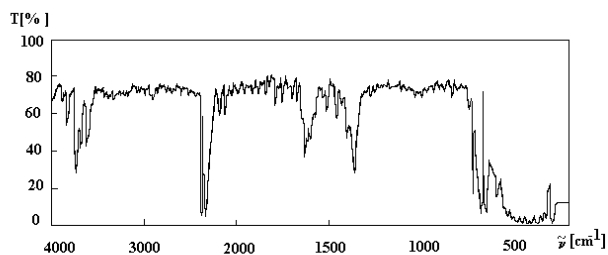
Figure 5. Gas products after the action of a positive dc corona discharge for the Mo–stainless steel combination of electrodes.
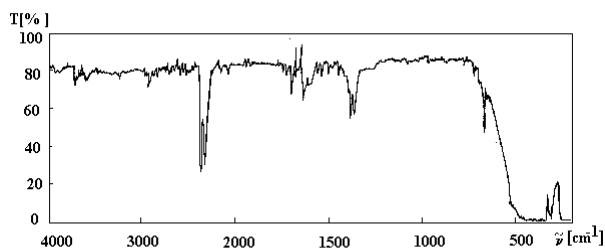
Figure 6. Gas products after the action of a negative dc corona discharge action for the copper–brass combination of electrodes.
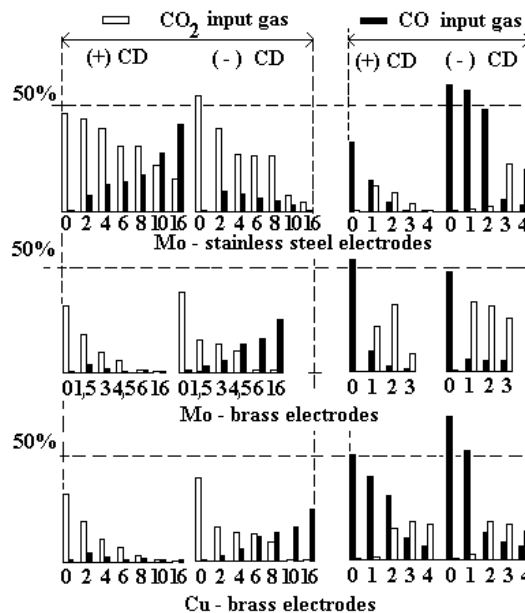
Figure 7. The relative changes in concentration of CO_2 and CO as percentages of the input concentration for both polarities of the dc corona discharge and with Mo–stainless steel, Mo–brass and Cu–brass combinations of materials used for the electrodes.

3.1.2. Minority gas components.
Very important information from measurements is the spectroscopic evidence about formation of stable –NCO intermediate radicals. This radical is formed during the decomposition of CO_2 and/or from CO when activated nitrogen is present in the gas mixture. The IR absorption bands of the –NCO radical in the gas phase are at 2270 and 2290 cm^{-1}. The presence of this radical in the gas after a discharge can be seen from the detailed IR absorption spectrum in figure 8.
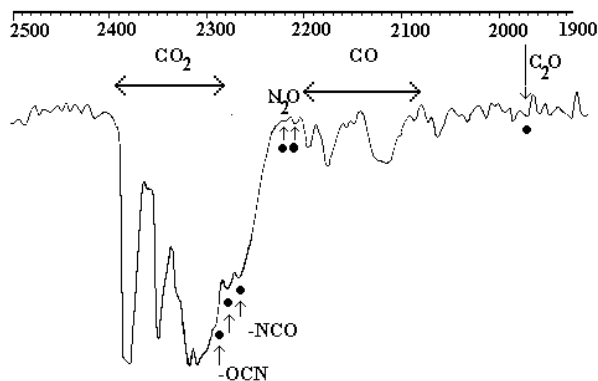
Figure 8. Detail of the IR absorption spectrum after the action of a dc corona discharge, in which evidence for the existence of –NCO radicals, N_2O and C_2O in the gas phase can be seen.
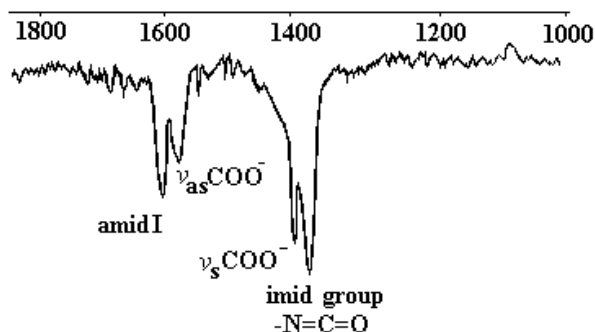
Figure 9. Detail of the IR absorption spectrum after the action of the negative corona discharge with copper and brass electrodes.

Because the –NCO radical is surface sensitive it forms organometallic compounds on the non-stressed electrode. Some of these compounds are known to influence the decomposition processes of CO_2, CO and NO gases. These surface products are based on OC–NCO and ON–NCO structural groups [32]. When these solid products with participation of the –NCO group in their structure are formed the wavenumbers of –NCO bands in IR absorption spectra are shifted to 2170 and 2215 cm^{-1} [33]. A part of the solid products can be decomposed due to electron bombardment and further cross linking. These processes are associated with the formation of small amounts of N_2O with absorption bands at 2220 and 2240 cm^{-1} and C_2O with absorption bands at 1950 cm^{-1}, as can be seen from figure 8.

In all mixtures containing CO and CO_2 the carboxylate ion –COO$^-$ is formed after the action of the discharge. This ion is present especially in surface products and for a negative polarity of the corona discharge as can be seen from figure 9. Also the carboxylate ion is very important for further production of organometallic complexes on the surfaces of electrodes.

C, C_2O (C+CO) and finally C_3O_2 (C_2O+CO) are formed by the CO decomposition processes. C_3O_2 named malonic acid anhydride, is a monomer which polymerizes differently for various polarities of the discharge. Created
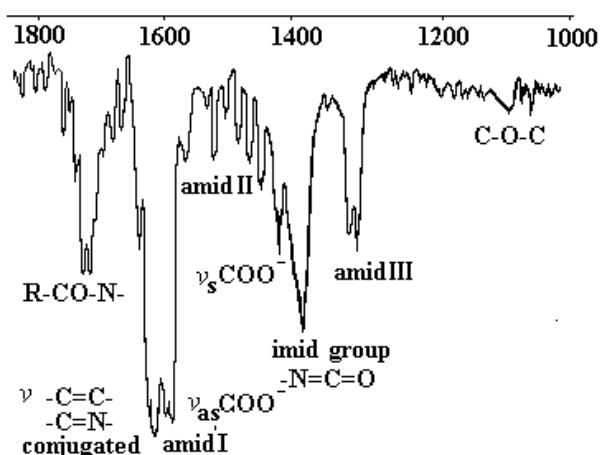
Figure 10. Detail of the IR absorption spectrum after the action of the positive corona discharge with molybdenum and stainless steel electrodes.

polymers are described in our previous work [16, 21]. For a positive polarity of the discharge the presence of malonic acid anhydride leads to a great increase in intensity of the broad band at 1650 cm^{-1} due to the conjugated –C=C– bond, as can be seen from figure 10.

Some of the intermediate products are similar to those proposed by Maezono and Chang [26] (C, C_2O, NCO and CO_3), but the final gas products that we have identified from IR absorption spectra are different. The main reason for this is the electrode material used. As we can see from figure 9, with a negative polarity of the discharge in the case of copper or brass electrodes the solid product is formed from gas products or intermediates. Owing to this the pressure of gas products permanently decreases, there is not equilibrium in the gas phase and the final efficiencies of CO and CO_2 removal processes increase. The final gas phase products (figure 9) contain the amino group and carboxylate ion, [NH$_2$–COO]$^-$. This is the radical of the unstable carbonic acid amide, but existing in a great variety of derivatives in the form of *negative ions*.

For the positive discharge polarity the gas products are based on the *positive ion* [NH$_2$–CO]$^+$, giving further amides and amino acids. This ion differ only by one oxygen from the previous one (for negative polarity), but give very different IR spectra. Typical is the presence of carbonyl and the amide III band and the absence of carboxylate ion bands, as can be seen from figure 10.

In the case of the stainless steel electrode the surface products are created very slowly. This leads to the development of a reaction equilibrium and limits the efficiency of removal of CO and CO_2. Owing to this the concentration of all intermediates is high.

3.2. The influence of the electrode material on the step by step development with time of products formed in the gas phase

The individual measurements of CO and CO_2 with air at atmospheric pressure were made for a longer period of time. That is why there are various differences in applied

Table 2. The step by step development with time of products for Mo and stainless steel electrodes.

Introduced gas CO_2–air mixture		Introduced gas CO–air mixture	
Positive polarity, 47.5% CO_2	Negative polarity, 55.7% CO_2	Positive polarity, 34.3% CO	Negative polarity, 55% CO
After 4.5 min CO 11.7% maximum CO_2 33.3% After 16 min Formation of –NCO radical and –COO⁻ ion CO_2 15.7% The surface reaction products are not bonded with the metal of the electrode	After 1.5 min CO 9.5% maximum CO_2 40.5% After 6 min Formation of –NCO radical After 16 min CO_2 14.6% The surface reaction products are not bonded with the metal of the electrode	After 1 min CO_2 12.3% maximum Formation of –NCO radical, –COO⁻ ion and carbonyl –CO After 3 min CO decreases to zero CO_2 decrease to 5.3% The surface reaction products are not bonded with the metal of the electrode	After 4 min CO decrease continually but not linear down to 4.1% CO_2 increase continually but not linear up to 21.5% The production of new gas products is very weak. The surface reaction product is not formed

Table 3. The step by step development with time of products for Mo and brass electrodes.

Introduced gas CO_2–air mixture		Introduced gas CO–air mixture	
Positive polarity, 33.3% CO_2	Negative polarity, 39.4% CO_2	Positive polarity, 50.0% CO	Negative polarity, 69% CO
After 1.5 min CO 4.4% maximum CO_2 19.4% After 3 min local maximum of –NCO, then a continuous rise until 16 min After 4.5 min CO_2 decreases to zero After 16 min CO_2 decreases to zero Surface reaction products are bonded to the metal of the electrode	After 1.5 min CO 4.5% maximum CO_2 16.4% After 3 min CO decreases to zero After 16 min CO_2 decreases to zero The new gas reaction product based on –NCO radical continuously but not linearly increases. The surface reaction products are not bonded with the metal of the electrode	After 3 min CO_2 19.2% maximum CO 11.3% formation of –NCO radical, –COO⁻ ion, carbonyl –CO and amino group –NH_2 After 4 min CO 6.5% CO_2 17.0% The surface reaction products are bonded to the metal of the electrode	After 3 min CO_2 18.6% maximum CO 13.6% The CO level decreases continually down to 1.9% after 6 min CO_2 increases continually to 11.3% after 6 min No other gas reaction products were formed

Table 4. The step by step development with time of products for copper and brass electrodes.

Introduced gas CO_2–air mixture		Introduced gas CO–air mixture	
Positive polarity, 35% CO_2	Negative polarity, 53.4% CO_2	Positive polarity, 54.7% CO	Negative polarity, 49% CO
After 1.5 min CO 1.5% maximum CO_2 15.6% After 4.5 min CO decreases to zero After 16 min CO_2 decreases to zero The new gas reaction products containing –NCO radical, –COO⁻ ion and amino acids continuously increase until 16 min after discharge The surface reaction products containing imide and imidoester groups are bonded to the metal of the electrode	After 1.5 min CO 5% maximum CO_2 33.8% After 4.5 min CO decreases to zero After 10 min CO_2 decreases to zero The new gas reaction product containing –NCO radical and –COO⁻ ion continuously but not linearly increases. Surface reaction products are bonded with the metal of the electrode	After 1 min CO_2 22.9% maximum CO 8.2% Formation of –NCO radical and –COO⁻ ion, carbonyl –CO and amino –NH_2 groups in gas products After 3 min CO_2 9.0% CO decreases to zero The surface reaction products containing imidoester and imidocarbonate groups are bonded to the metal of the electrode	After 2 min CO_2 34.2% maximum CO 6.4% After 3 min CO_2 26.6% CO 5.4% In reaction products, amino acids dominate. The surface reaction products had acid character and are bonded to the metal of the electrode
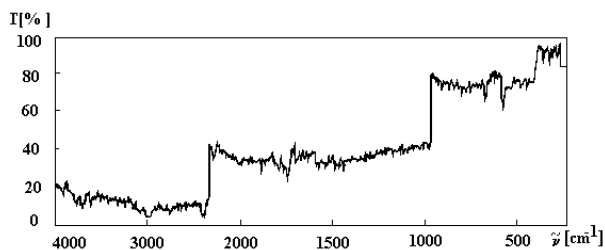
Figure 11. The IR absorption reflection spectrum of the stainless steel non-stressed electrode surface in the case of a positive corona discharge with electrode materials molybdenum and stainless steel and input gas CO_2.
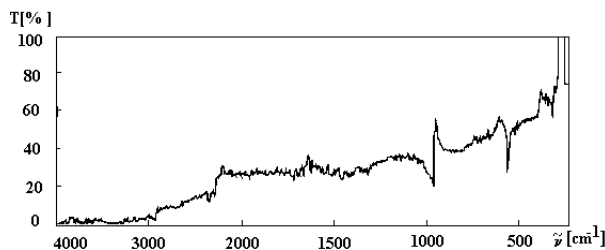
Figure 12. The IR absorption reflection spectrum of the stainless steel non-stressed electrode surface in the case of a negative corona discharge with electrode materials molybdenum and stainless steel and input gas CO_2.
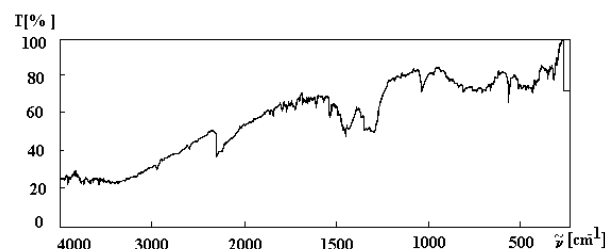
Figure 13. The IR absorption reflection spectrum of the brass non-stressed electrode surface in the case of a positive corona discharge with electrode materials molybdenum and brass and input gas CO_2.
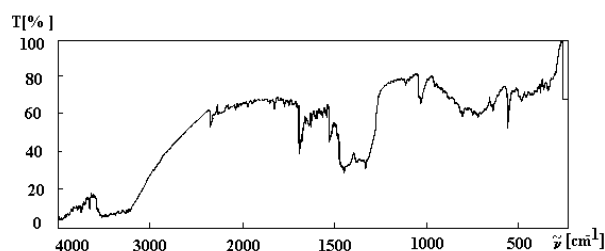
Figure 14. The IR absorption reflection spectrum of the brass non-stressed electrode surface in the case of a negative corona discharge with electrode materials molybdenum and brass and input gas CO_2.

parameters (input ratios between air and CO and CO_2 and residence time). The measurements are performed for three combinations of materials. Owing to the method applied, it was possible to evaluate step by step the development with time of products. The concentrations of known gas
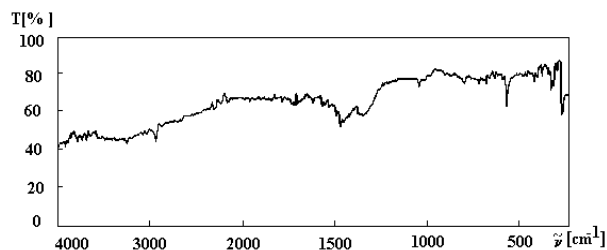
Figure 15. The IR absorption reflection spectrum of the brass non-stressed electrode surface in the case of a positive corona discharge with electrode materials copper and brass and input gas CO_2.
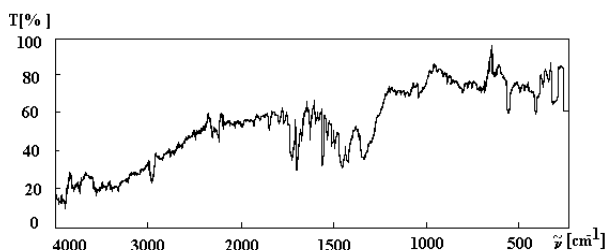
Figure 16. The IR absorption reflection spectrum of the brass non-stressed electrode surface in the case of a negative corona discharge with electrode materials copper and brass and input gas CO_2.

components are expressed as percentages. For products with unknown extinction coefficients we used the time of first appearance of their bands in IR spectra. To provide a more detailed overview of the described effects, we have collected results into tables 2–4 for each combination of materials.

3.3. Surface products

For each measurement we have analysed the surface of the non-stressed electrode. As analysing method we have used IR absorption reflection spectrometry. The reflection spectra for various materials of the non-stressed electrode, both polarities of the discharge and for CO_2 input gas are in figures 11–16. The surfaces of the electrodes for CO input gas have similar characters to those in the case of CO_2, only the surface layer is fully developed in a shorter period of time.

The surface products differ with the polarity of the discharge and the material of the non-stressed electrode.

(i) For the input CO_2–air and CO–air mixtures and *negative polarity* of the discharge the surface products contain the following functional groups: the OC–NCO group in *cis* configuration, which may lead to the formation of imides

OC-NCO group

1871
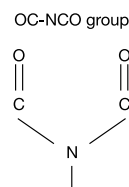
the OC–CCO groups in *cis* configuration, also known as malonic acid anhydride,
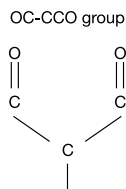
OC-CCO group

leading to the formation of chelates of β-dicarbone compounds; the –CCO group, which may create, together with OC–NCO, the pyrrole ring

-CCO group OC-NCO group pyrrol ring
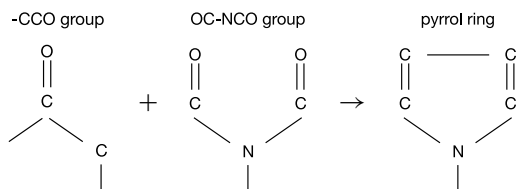
the carboxylate ion –COO⁻ and its dimer (–COO⁻)$_2$

carboxylate ion and its dimer
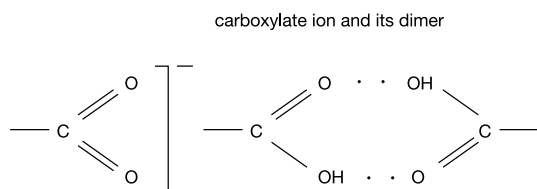
–NH$_2$-COO⁻ which leads to the formation of urethanes (carbamates) and, after stabilization by polymerization, polyurethane

- NH$_2$-COO-group
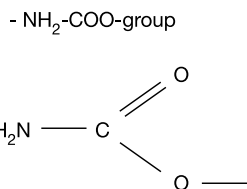
and –(HNCO)$_2$ which leads to the formation of oxamidato complexes.

(ii) For the input CO$_2$–air and CO–air mixtures and *positive polarity* of the discharge the surface products contain following functional groups: the OC–NCO group in *cis* configuration, which leads later to the formation of imides. Similarly to the case with negative polarity, the pyrrole ring is created from OC–NCO and –CCO groups

-CCO group OC-NCO group pyrrol ring
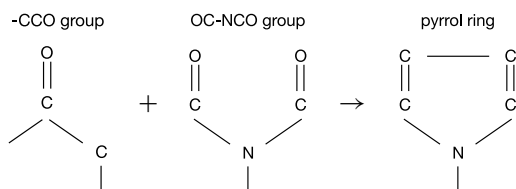
–(HNCO)$_2$ which leads to the formation of oxamidato complexes

oxamidato complex
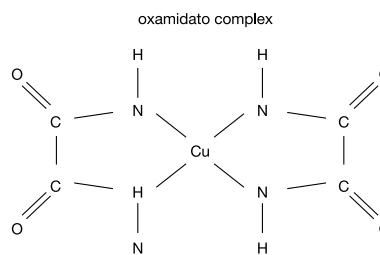
and –NH$_2$–CO⁻ leading the formation of amino acids, mostly α alanine, serine and aspartic acids

α-alanine, serine and aspartic acid

alanine

serine

aspartic acid
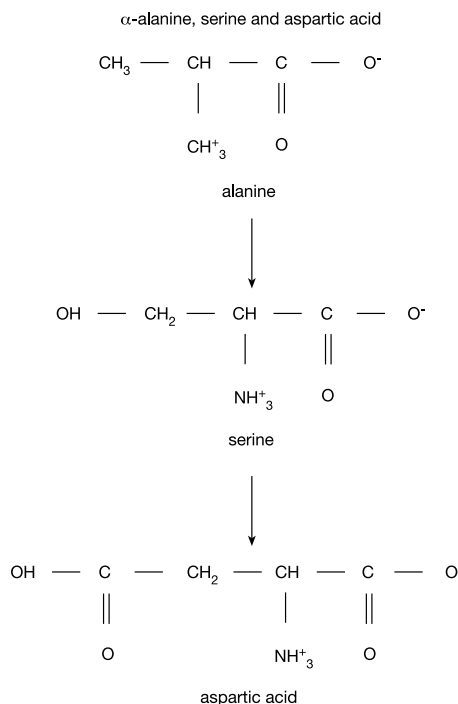
The surface reaction products are not bonded with the metal of the non-stressed electrode for the Mo–stainless steel combination of electrodes, but are bonded to the material of the non-stressed electrode for Mo–brass and Cu–brass combinations of electrodes. For non-stressed anodes containing copper the polynuclear metal complexes formed on the electrode surface due to the action of the corona discharge act as catalysts with photochemical activity [35].

4. Conclusions

The results from the studied combinations of electrodes, gas mixtures and times of action of the corona show the following.

(i) From the point of view of decreasing the concentration of CO$_2$ the highest efficiency of removal is for a negative corona discharge with Cu and brass electrodes; the lowest efficiency of removal is for a positive corona discharge with Mo and stainless steel electrodes.

(ii) From the point of view of decreasing the concentration of CO the highest efficiency of removal is for

a positive corona discharge with Cu and brass electrodes; the lowest efficiency of removal is for a negative corona discharge with Mo and brass electrodes.

The discharges with electrodes made from Mo and brass in negative polarity and with electrodes of Cu and brass in positive polarity were typical, with high amounts of surface reaction products. The negative corona discharge with Mo and stainless steel electrodes acts practically without surface reaction products. The development of surface products is based on the following radicals formed by the discharge:

(i) the NCO radical, which is changed to more complex formations such as

(ii) OC–CCO (leading to production of chelates of β-dicarbone compounds),

(iii) OC–NCO and ON–NCO in *cis* configuration (leading to the formation of polyimides),

(iv) $(HNCO)_2$ (leading to the production of oxamidato complexes),

(v) the dimer of $(COO^-)_2$ (leading to the formation of acids or esters),

(vi) $-NH_2-CO-$, leading to the formation of amino acids (mostly α alanine, serine and aspartic acids) and

(vii) $-NH_2-COO-$, leading to the formation of urethanes.

The necessary $-NH_2$ group is formed by the discharge in the following steps:

(i) a change of CO_2 configuration from O=C=O to $-COO^-$ due to the presence of water and an electric field,

(ii) the production of excited nitrogen by the discharge,

(iii) incorporation of nitrogen into $-COO^-$, exchange of oxygen with nitrogen and creation of $-NCO$ radicals and

(iv) reaction of $-NCO$ radicals with H_2O, formation of the $-HN_2-COO^-$ functional group with a negative polarity of the discharge and $-HN_2-CO^+$ with a positive polarity of the discharge:

$$-NCO + H_2O \rightarrow -N\,H_2-CO\,O^-.$$
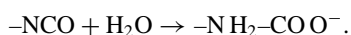
For separation of CO_2 from flue gases, the following methods are used:

(i) wet absorption of CO_2 in an amine or alkaline type of solvent,

(ii) dry absorption of CO_2 by zeolite-packed bed filters and

(iii) membrane separation of CO_2 by use of a polymer membrane.

Separated CO_2 will be liquefied and stored in the deep sea.

An alternative method for removal and fixation of CO_2 and CO could be to use corona discharges with surface active material on the electrodes in the presence of water. The method gives high efficiencies for the removal process. Although the gas intermediates (mostly amines) can be toxic, the final gas, liquid and solid products are not harmful. The method associates decomposition and activation processes in the volume of the discharge with synthesis of the final solid products on the surface of the electrodes. The activation factors for volume processes are mostly electrons, but for surface processes, with a great probability, light.

Acknowledgments

References

[1] Böhm J 1982 *Electrostatic Precipitators* (Amsterdam: Elsevier)

[2] Chang J S 1993 *Non-Thermal Plasma Techniques for Pollution Control (NATO ASI Series 34A)* ed B M Penetrante and S E Schultheis (Berlin: Springer) pp 1–32

[3] Civitano L 1993 *Non-Thermal Plasma Techniques for Pollution Control (NATO ASI Series 34B)* ed B M Penetrante and S E Schultheis (Berlin: Springer) pp 103–30

[4] Mizuno A, Chakrabarti A and Okazaki K 1993 *Non-Thermal Plasma Techniques for Pollution Control (NATO ASI Series 34B)* ed B M Penetrante and S E Schultheis (Berlin: Springer) pp 165–86

[5] Kogelschatz U and Eliasson B 1996 Greenhouse gas plasma chemistry in silent discharges *Book of Contributed Papers from Hakone V, Milovy, Czech Republic, September 2–4, 1996* (Brno: Universitas Masarykiana Brunensis) pp 47–51

[6] Yamamoto T, Lawness P A, Owen M K, Ensor D S and Boss C 1993 *Non-Thermal Plasma Techniques for Pollution Control (NATO ASI Series 34B)* ed B M Penetrante and S E Schultheis (Berlin: Springer) pp 223–38

[7] Paur H R 1993 *Non-Thermal Plasma Techniques for Pollution Control (NATO ASI Series 34B)* ed B M Penetrante and S E Schultheis (Berlin: Springer) pp 77–89

[8] Tevault D E 1987 *Plasma Chem. Plasma Processing* **7** 231–42

[9] Rosswall T 1991 *Environmental. Sci. Technol.* **25** 567–73

[10] Mizuno A, Ito H and Yoshida H 1988 *Proc. Inst. Electrostatics, Japan* (Tokyo: IEJ ESA) pp 337–40

[11] Wagner H E and Huczko A 1991 *Proc. 10th Int. Symp. on Plasma Chemistry, Bochum, August 1991* (Bochum: RU) 3.2–18, p 1

[12] Huczko A and Resztak A 1989 *Proc. 9th Int. Symp. on Plasma Chemistry, Pugnochiuso* ed R d'Agostino (Bari: Universita Degli Studi di Bari) p 1685

[13] Huczko A, Resztak A and Opalinska T 1989 *Proc. HAKONE II, Kazimierz* (Lublin: LTU) p 110

[14] Boukhalfa N M, Goldman A, Goldman M and Sigmond R S 1987 *Proc. 8th Int. Symp. on Plasma Chemistry, Tokyo* (Tokyo: ISPC) p 787

[15] Sigmond R S, Goldman A and Goldman M 1992 *Proc. 10th Int. Conf. on Gas Discharges and Their Applications, Swansea* (Swansea: W T Williams) p 330

[16] Tegelhofová M 1981 *CSc disertation* Bratislava

[17] Morvová M and Morva I 1990 *Proc. 8th Symp. on Elementary Processes and Chemical Reactions in Low Temperature Plasma, Stará Lesná* (Bratislava: JSMF & MFFUK) p 45

[18] Gardinger P S and Craggs J D 1977 *J. Phys. D: Appl. Phys.* **10** 1003

[19] Gardinger P S, Moruzzi J L and Craggs J D 1978 *J. Appl. Phys.* **11** 237

[20] Alger S R and Rees J A 1977 *J. Phys. D: Appl. Phys.* **10** 957

[21] Tegelhofová M and Martišovitš V 1986 *Acta Phys. Slovaca* **36** 164
[22] Sobek V and Morvová M 1990 *Acta Phys. Universitatis Comeniana* **31** 33
[23] Tegelhofová M and Martišovitš V 1979 *Acta Phys. Slovaca* **29** 103
[24] Eliason B, Simon F G and Egli W 1993 *Non-Thermal Plasma Techniques for Pollution Control (NATO ASI Series 34B)* ed B M Penetrante and S E Schultheis (Berlin: Springer) pp 321–37
[25] Hayash H, Beuthe T G, Nagay K and Jen Shih Chang 1992 *Proc. 10th Int. Conf. on Gas Discharges and Their Applications, Swansea* (Swansea: W T Williams) p 774
[26] Maezono I and Chang Jen-Shih 1990 *IEEE Trans. Indust. Appl.* **26** 651–5
[27] Weiss H R 1985 *Proc. Int. Conf. on Plasma Chemistry* vol 2 (Eindhoven: ISPC) pp 383–8
[28] Jogan K, Mizuno A, Yamamoto T and Chang J S 1993 *IEEE Trans. Indust. Appl.* **29** 876–81
[29] Morvová M 1988 *Proc. 7th Symp. Elementary Processes and Chemical Reactions in Low Temperature Plasma, Stará Turá-Dubník* (Bratislava: JSMF & MFFUK) pp 80–95
[30] Tegelhofová M and Martišovitš V 1983 *Acta Phys. Slovaca* **33** 25–35
[31] Wozniak A, Czech T, Mizeraczyk J and Fujii K 1989 *Proc. HAKONE II, Kazimierz* (Lublin: LTU) p 118
[32] Cooper W F and Hershberger J F 1992 *J. Phys. Chem.* **96** 771–5
[33] Tanase T, Nitta S, Yoshikawa S, Kobayashi K, Sakurai T and Yano S 1992 *Inorg. Chem.* **31** 1058–62
[34] Lloret F, Julve M, Faus J, Ruiz R, Castro I, Mollar M and Philoche-Levisalles M 1992 *Inorg. Chem.* **31** 784–91
[35] Masao Kaneco and Eishun Tsuchida 1981 *J. Polym. Sci. Macromol. Rev.* **16** 397–522
[36] Veisová M and Skalný J 1977 *Acta FRNUC – Formatio et protectio naturae III* pp 183–94
[37] Morvová M, Morva I, Sobek V and Èordáš J 1991, Czecho-slovak patent 274860
[38] Higashi M, Sugaya M, Ueki K and Fujii K 1985 *Proc. Int. Conf. on Plasma Chemistry* vol 2 (Eindhoven: ISPC) pp 366–71
[39] Jolly S, Saussey J and Lavalley J C 1994 *Catalysis Lett.* **24** 141–6
[40] Holly S and Sohar P 1975 *Absorption Spectra in Infrared Region* (Budapest: Ákádemiai kiadó) p 144
[41] Haslam J and Willis H A 1972 *Identification and Analysis of Plastics* (London: Iliffe)
[42] Hummel D O and Scholl F 1978 *Atlas of Polymer and Plastic Analysis* vol 1 (Munich: Hanser)
[43] Bentley F F, Smithson L D and Rozek A L 1968 *Infrared Spectra and Characteristic Frequencies 700–300 cm^{-1}* (New York: Interscience)
[44] Nakamoto K 1966 *Infrared Spectra of Inorganic and Coordination Compounds* (Moscow: MIR) (in Russian)